

Heating a Distant Galaxy Cluster by Giant X-ray Cavities and Large-Scale Shock Fronts

B. R. McNamara¹, P. E. J. Nulsen^{2,3}, M. W. Wise⁴, D. A. Rafferty¹, C. Carilli⁵, C. L. Sarazin⁶, & E. L. Blanton^{6,7}

¹ Astrophysical Institute and Department of Physics & Astronomy, Ohio University, Clipper Laboratorie, Athens, OH 45701

² Harvard-Smithsonian Center for Astrophysics, 60 Garden St., Cambridge, MA

³ On leave from the University of Wollongong

⁴ MIT Center for Space Research

⁵ National Radio Astronomy Observatory, Very Large Array, Socorro, NM

⁶ Astronomy Department, University of Virginia, Box 3818, Charlottesville, VA 22903

⁷ Institute for Astrophysical Research, Boston University

Most of the baryons in galaxy clusters reside between the galaxies in a hot, tenuous gas¹. The densest gas in their centers should cool and accrete onto giant central galaxies at rates of 10 – 1000 solar masses per year¹. However, no viable repository for this gas has been found¹. This paradigm changed abruptly when new X-ray observations showed far less cooling below X-ray temperatures than expected². Consequently, most of the gas must be heated and maintained above $\simeq 2$ keV³. The most promising heating mechanism concerns powerful radio jets emanating from supermassive black holes in central cluster galaxies⁴. Here we report the discovery of giant cavities and shock fronts in a distant ($z = 0.22$) cluster caused by an interaction between a radio source and the hot gas surrounding it. The energy involved is $\sim 6 \times 10^{61}$ erg, the most powerful radio outburst known. This is enough energy to quench a cooling flow for several Gyr, and to provide $\sim 1/3$ keV per particle of heat to the surrounding cluster.

Cavities with diameters ranging from a few to a few tens of kpc have been found in the hot gas surrounding nearly two dozen galaxies, groups, and clusters⁵. Their enthalpy (free energy), which ranges between $pV = 10^{55} – 10^{60}$ erg, scales in proportion to the cooling X-ray luminosity and the radio power of the host system⁵. The cavities and weak shocks in half of these systems are currently injecting enough energy into the hot gas to balance radiation

losses (cooling)^{6,7}, but it is unclear whether they can quench cooling over longer timescales. Systems without cavities today could have been heated in the past by powerful but relatively rare outbursts⁸. However, prior to the discoveries of large scale cavities and shocks discussed here and in a companion paper⁹, little evidence existed to support this conjecture.

Giant cavities, each roughly 200 kpc in diameter, were found in a *Chandra* X-ray image the optically poor cluster MS0735.6+7421 (Fig. 1). The center of the cluster harbors a cD galaxy that hosts a radio source roughly 550 kpc in size. The radio lobes fill the cavities suggesting, as in other clusters, that the gas was displaced and compressed by the advancing radio source. Both the cavities and the radio source dwarf the cD galaxy, which is itself a member of the class of the largest galaxies in the Universe.

The average pressure surrounding the cavities (Fig. 2) is $P \simeq 6 \times 10^{-11}$ erg cm⁻³. The work required to inflate each cavity against this pressure is $pV \approx 10^{61}$ erg. Their enthalpy can approach $4pV$ per cavity, depending on the equation of state of the gas filling them, giving a value of $\approx 8 \times 10^{61}$ erg. To place this figure in perspective, it exceeds the enthalpy of the cavities in the Perseus cluster⁶, Cygnus A⁵, and M87⁷ by roughly 250 times, 15 times, and more than four orders of magnitude, respectively. Only the energy of the recently-discovered shock front in Hydra A⁹ falls within an order of magnitude of this value.

The bright elliptical region surrounding the X-ray cavities strongly resembles the hot cocoon of jet-powered radio source models^{10,11}. In this interpretation, the relatively sharp edge of the cocoon lies at the location of an enveloping shock (Fig. 3). The two red “hot spots” in Fig. 4 show that the gas near the cavities is being heated by the shocks. By contrast, the gas surrounding the cavities in other systems such as Hydra A⁴ and Perseus⁶ is relatively cool, suggesting that buoyancy, not excess pressure, is driving their outward advance.

The shock properties were determined using a spherical hydrodynamic model of a point explosion at the center of an initially isothermal, hydrostatic atmosphere (Fig. 3). The age and driving energy of the shock are $t_s \simeq 1.04 \times 10^8$ yr and $E_s \simeq 5.7 \times 10^{61}$ erg, respectively. The energy is proportional to the preshock temperature, which probably exceeds 5 keV. The spherical model underestimates the shocked volume, tending to underestimate total energy. Furthermore, since the cavities occupy a large fraction of the cocoon, they appear to be driving the shock, which undermines to some degree our assumption of a point explosion. Nevertheless, we expect the energy of the outburst to be within a factor ~ 2 of the model estimate, and more likely to exceed it.

The shock energy is reassuringly close to the cavity enthalpy, and we adopt the shock energy as the probable value. The average jet power of the outburst is then $P_s = E_s/t_s \simeq 1.7 \times 10^{46}$ erg s⁻¹, comparable to a powerful quasar radiating at the Eddington limit of a $\sim 2 \times 10^8$ M_⊙ black hole. The flux density of the radio source at 1.4 GHz is 21 mJy¹², corresponding to a monochromatic luminosity of 4×10^{40} erg s⁻¹, several orders of magnitude fainter than powerful quasars¹³. The ratio of average jet power to monochromatic radio power is $\sim 10^5$, enormously larger than the generally accepted factor of 10 to 100^{13,14} for powerful radio sources. Evidently, even relatively faint radio sources can be mechanically powerful⁵. Bright radiation from an active quasar is surprisingly absent both in the optical and X-ray

bands. However, the cD harbors a $\sim 10^{42}$ erg sec $^{-1}$ optical emission nebula extending over its inner 20 kpc¹⁵, which are commonly found in cooling flows.

This outburst released enough energy to quench a $200 M_{\odot}$ yr $^{-1}$ cooling flow for several Gyr, assuming all of the energy is deposited within the ~ 50 kpc cooling region of the cluster. The central cooling time of the gas is roughly 1 Gyr, so the cooling that ensues could establish a feedback cycle of heating and cooling driven by accretion onto the central black hole^{8,16,17}. A similar process occurring in other clusters would in principle maintain the observed levels of hot gas with short cooling times, molecular gas¹⁸, and star formation¹⁹ in cD galaxies, while preventing the development of a more massive, steady cooling flow^{1,20}. The existence of bright nebular emission located in the the cD galaxy is consistent with this picture¹⁵.

Much of the energy is, however, leaving the cooling region, bound for the cluster's outskirts. The gas mass $5.5 \pm 0.7 \times 10^{13} M_{\odot}$ within one Mpc is being heated at the level of $\simeq 1/3$ keV per particle. This one event alone then provides a substantial fraction of the 1 – 3 keV per particle of heat required to raise the entropy above the level of gravity alone (preheating)²¹. For a bolometric, unabsorbed X-ray luminosity of 1.1×10^{45} erg s $^{-1}$ and a mean temperature of 4.5 keV, the cluster departs upward in luminosity by several times from the relatively tight correlation between X-ray luminosity and gas temperature^{22,20}. Since the shock power exceeds the cluster's X-ray luminosity by 15 times, the shock is surely capable of causing this departure. The time required to radiate away the shock energy $\gtrsim E_s/L_x \sim 2$ Gyr is a substantial fraction of the age of the cluster. Therefore, this outburst will leave a persistent mark on the temperature and luminosity of the cluster, even after the cavities have disappeared. Assuming this event is not unique, substantial heating must have occurred recently in clusters, not just during an early preheating epoch²¹. Events of this nature would complicate the use of X-ray temperature and luminosity functions to probe the large scale structure and cosmology²².

The titanic proportion of this event suggests it was powered by accretion onto a black hole. Equating the shock energy to $0.1 M c^2$ gives an estimate of the minimum accreted mass required to power the burst of $M \simeq 3 \times 10^8 M_{\odot}$, itself the mass of a supermassive black hole. The relationship between galactic bulge luminosity and black hole mass²³ predicts a $\sim 10^9 M_{\odot}$ black hole resides there (assuming the cD's absolute visual magnitude within a 35 kpc diameter is -22.4 ²⁴). Evidently the central black hole accreted a substantial fraction of its own mass in only 10^8 yr, a remarkable growth rate for such a large black hole. While a similar line of reasoning would apply to quasars, their ages and average jet powers have not been measured directly. Such a rapid rate of growth may be difficult to reconcile with the small scatter in the black hole mass to bulge mass relation²⁵, and is at variance with the view that the most massive black holes have evolved slowly in the recent past²⁶.

Finally, the magnetic field strengths in clusters are typically a few μG ²⁷, and evidence is growing for the existence of large-scale, intergalactic fields^{28,29}. These fields could be generated and dispersed by outflows from supermassive black holes^{28,29}. The equivalent magnetic field strength corresponding to the energy density within the cavities is $\sim 100 \mu\text{G}$, considerably larger than the accumulated field strengths in clusters²⁷. Therefore, a plausibly

small fraction of the total energy of this one radio outburst alone channeled into magnetic field would magnetize the cluster.

1. Fabian, A. C. Cooling Flows in Clusters of Galaxies, *Ann. Rev. Astron. Astrophys.* **32**, 277-318 (1994)
2. Peterson, J. R. *et al.* High-Resolution X-Ray Spectroscopic Constraints on Cooling-Flow Models for Clusters of Galaxies. *Astrophys. J.* **590**, 207-224 (2003)
3. Fabian, A. C., Mushotzky, R. F., Nulsen, P. E. J., Peterson, J. R. “On the soft X-ray spectrum of cooling flows.” *Mon. Not. R. Astr.* **321**, 20 (2001)
4. McNamara, B. R. *et al.* Chandra X-Ray Observations of the Hydra A Cluster: An Interaction between the Radio Source and the X-Ray-emitting Gas. *Astrophys. J. Lett.* **534**, 135-138 (2000)
5. Bîrzan, L. *et al.* A Systematic Study of Radio-induced X-Ray Cavities in Clusters, Groups, and Galaxies. *Astrophys. J.* **607**, 800-809 (2004)
6. Fabian, A. C. *et al.* A deep Chandra observation of the Perseus cluster: shocks and ripples. *Mon. Not. R. astr.* **344**, 43-47 (2003)
7. Forman, W. *et al.* Reflections of AGN Outbursts in the Gaseous Atmosphere of M87. *Astrophys. J.* Submitted (2004)
8. Soker, N. *et al.* A Moderate Cluster Cooling Flow Model. *Astrophys. J.* **549**, 832-839 (2001)
9. Nulsen, P. E. J. *et al.* The Cluster-Scale AGN Outburst in Hydra A. *Astrophys. J.* Submitted (2004)
10. Scheuer, P. A. G. Models of extragalactic radio sources with a continuous energy supply from a central object. *Mon. Not. R. astr.* **166**, 513-528 (1974)
11. Heinz, S., Reynolds, C. S., & Begelman, M. C. X-Ray Signatures of Evolving Radio Galaxies. *Astrophys. J.* **501**, 126-136 (1998)
12. Condon, J. J. *et al.* The NRAO VLA Sky Survey. *Astron. J.* **115**, 1693-1716 (1998)
13. Bicknell, G. V., Dopita, M. A., & O’Dea, C. P. Unification of the Radio and Optical Properties of Gigahertz Peak Spectrum and Compact Steep-Spectrum Radio Sources. *Astrophys. J.* **485**, 112-124 (1997)
14. De Young, D. S. On the relation between Fanaroff-Riley types I and II radio galaxies. *Astrophys. J. Lett.* **405**, 13-16 (1993)
15. Donahue, M., Stocke, J. T., & Gioia, I. M. Distant cooling flows. *Astrophys. J.* **385**, 49-60 (1992)
16. Churazov, E. *et al.* Evolution of Buoyant Bubbles in M87. *Astrophys. J.* **554**, 261-273 (2001)
17. Churazov, E. *et al.* Cooling flows as a calorimeter of active galactic nucleus mechanical power. *Mon. Not. R. astr.* **332**, 729-734 (2002)
18. Edge, A. C. The detection of molecular gas in the central galaxies of cooling flow clusters. *Mon. Not. R. astr.* **328**, 762-782 (2001)
19. McNamara, B. R. & O’Connell, R. W. Star Formation in Cooling Flows in Clusters of Galaxies. *Astron. J.* **98**, 2018-2043 (1989)

20. Donahue, M. & Stocke, J. T. *ROSAT* Observations of Distant Clusters of Galaxies. *Astrophys. J.* **449**, 554-566 (1995)
21. Wu, K. K. S., Fabian, A. C., & Nulsen, P. E. J. Non-gravitational heating in the hierarchical formation of X-ray clusters *Mon. Not. R. astr.* **318**, 889-912 (2000)
22. Markevitch, M. The LX-T Relation and Temperature Function for Nearby Clusters Revisited *Astrophys. J.* **504**, 27-34 (1998)
23. Gebhardt, K. *et al.* A Relationship between Nuclear Black Hole Mass and Galaxy Velocity Dispersion. *Astrophys. J. Lett.* **539**, 13-16 (2000)
24. Stocke, J. T. *et al.* The Einstein Observatory Extended Medium-Sensitivity Survey. II - The optical identifications. *Astrophys. J. Suppl.* **76**, 813-874 (1991)
25. Ferrarese, L. & Merritt, D. A Fundamental Relation between Supermassive Black Holes and Their Host Galaxies. *Astrophys. J.* **539**, L9-L12 (2000)
26. Heckman, T. M. *et al.* Present-Day Growth of Black Holes and Bulges: the SDSS Perspective. *Astrophys. J.* in press (2004) astro-ph/0406218
27. Clarke, T. E., Kronberg, P. P., & Böhringer, H. A New Radio-X-Ray Probe of Galaxy Cluster Magnetic Fields. *Astrophys. J. Lett.* **547**, 111-114 (2001)
28. Kronberg, P. P. *et al.* Magnetic Energy of the Intergalactic Medium from Galactic Black Holes. *Astrophys. J.* **560**, 178-186 (2001)
29. Furlanetto, S. R. & Loeb, A. Intergalactic Magnetic Fields from Quasar Outflows. *Astrophys. J.* **556**, 619-634 (2001)

All correspondence should be addressed to Brian R. McNamara, Astrophysical Institute and Dept. of Physics & Astronomy, Ohio University, Clippinger Labs, Athens, OH 45701

B.R.M thanks Gus Evrard, Dave De Young, and Joe Shields for helpful discussions. This work was supported by a NASA Long Term Space Astrophysics grant, a Chandra Archival Research grant, a Chandra Guest Observer grant, and a contract from the Department of Energy through the Los Alamos National Laboratory.

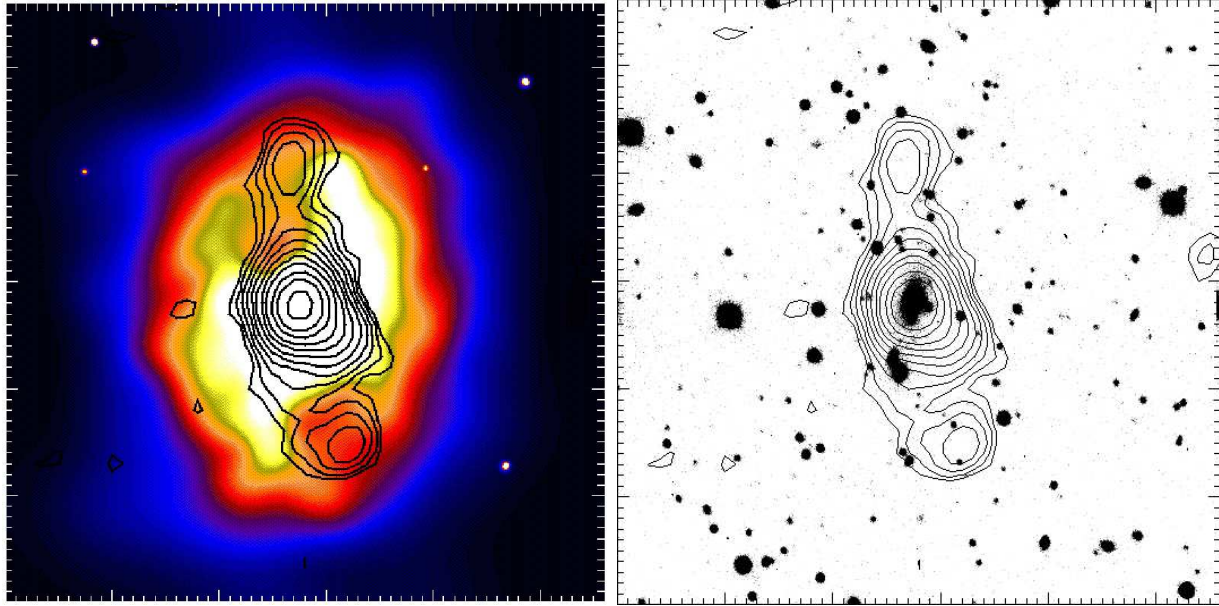


Figure 1 The relationships between the X-ray, radio, and optical emission of the cluster. The smoothed X-ray image (left) and optical image (right) are superposed with the 1.4 GHz radio contours. The 40 ksec X-ray image was obtained with the *Chandra* X-ray Observatory on 1 December 2003. Approximately 75000 useful X-ray photons were detected. The X-ray surface brightness depressions (cavities) are between 10% – 20% fainter than the surrounding X-ray emission to the north and south of the center. Most of the cluster’s emission emerges from an elliptical structure bounded by a shock front. We assume a flat cosmology with $H_0 = 70 \text{ km s}^{-1} \text{ Mpc}^{-1}$ and $\Omega = 0.3$, corresponding to a ratio of linear to angular size of $3.5 \text{ kpc arcsec}^{-1}$ at the redshift of the cluster throughout this paper.

The $\simeq 4$ arcsec resolution radio map was made with the Very Large Array telescope in the C configuration. The cavities are filled with radio emission. Assuming spherical cavities whose edges lie at the midpoints of the rims, each is roughly an arcmin in diameter (200 kpc) centered approximately 125 kpc to the north-east and to the south-west of the cluster center RA = 07 41 44.0, Dec = +74 14 38.3, (J2000). The radio contour levels are $2 \times 10^{-4} \times (-1, 1, 1.4, 2, 2.8, 4, 5.7, 8, 11, 16, 22, 32)$ Jy/beam. The radio contour levels on the visual image are $2 \times 10^{-4} \times (-1, 1, 1.4, 2, 2.8, 4, 5.7, 8, 11, 16, 22)$ Jy/beam. The cD’s *R*-band surface brightness peaks at its center at roughly 19.5 mag arcsec $^{-2}$ and diminishes with radius in $r^{1/4}$ -law fashion, reaching 25.5 mag 105 kpc. Each image is 250×250 arcsec (875×875 kpc) on a side.

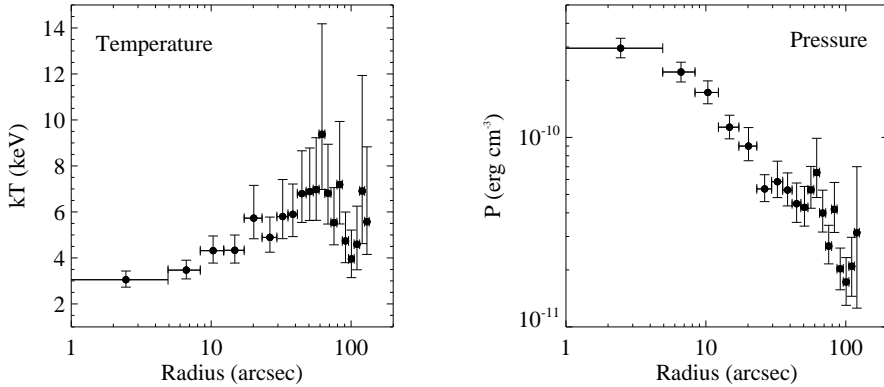


Figure 2 Projected temperature and pressure profiles of the cluster gas. The vertical error bars are 90% confidence intervals, and the horizontal bars represent the bin sizes. The spectra used to construct these profiles were extracted from the X-ray image in circular apertures centered on the cD. The spectra were modeled as thermal emission from a single temperature plasma of uniform metallicity, attenuated by the foreground column of neutral hydrogen in our Galaxy. The average metallicity of the gas was found to be 0.4 times the solar value. The temperature and pressure profiles are complex. The coolest gas located in the center of the cluster is roughly 3 keV. The temperature rises with increasing radius reaching an average of about 7 keV between 50 and 80 arcsec. Beyond 80 arcsec the temperature drops to roughly 5 keV, although the level of this drop is uncertain. The pressure is highest in the center 3×10^{-10} erg cm $^{-3}$, and declines smoothly with radius in roughly power law fashion until reaching a radius of roughly 70 arcsec. The pressure there rises abruptly at the shock front.

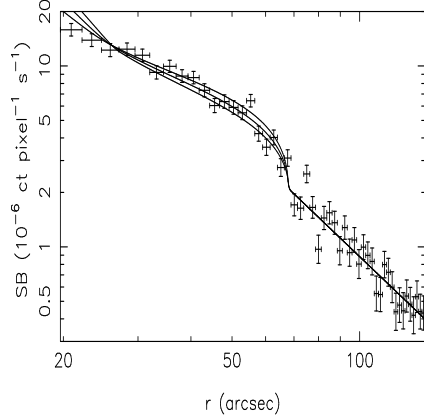


Figure 3 Projected 0.5–7.5 keV radial surface brightness profile of the cocoon region compared to shock model predictions. The profile was measured in 30° sectors to the east and west, along the minor axis of the ellipse (PA’s $90^\circ - 120^\circ$ and $270^\circ - 300^\circ$), where the shock is relatively uniform. The feature at a radius of 69 arcsec (240 kpc) is consistent with being a weak shock. The surface brightness beyond is well fitted by the power law, $r^{-\beta}$ with $\beta = 2.24 \pm 0.29$ (90%). To be consistent with the surface brightness profile beyond the shock, the gas density initially has $\rho(r) \propto r^{-\eta}$, with $\eta = 1.62$, and the gravitational field was chosen to make the undisturbed atmosphere hydrostatic. The model assumes the temperature of the unshocked gas is 5 keV. The *Chandra* 0.5 – 7.5 keV response was computed using XSPEC and an absorbed mekal model with foreground column density $3.49 \times 10^{20} \text{ cm}^{-2}$, redshift 0.216 and abundance 0.4 times solar (results are insensitive to these parameters). Model surface brightness profiles are scaled to match the observed profile in the unshocked region. The three lines represent model profiles for shock Mach numbers of 1.41 and 1.41 ± 0.07 (increasing Mach number from bottom to top). The greatest source of uncertainty in the age is the preshock temperature, since the Mach number is not strongly model-dependent (in particular, if the cocoon is axially symmetric, the age estimate is not sensitive to projection effects). The temperature increase for a shock of this magnitude is expected to be roughly 30% above the preshock value. This jump is consistent with the data, but the uncertainty in the pre- and post-shock temperatures are too large to further constrain the shock properties. The vertical error bars are 90% confidence intervals, and the horizontal bars represent the bin sizes.

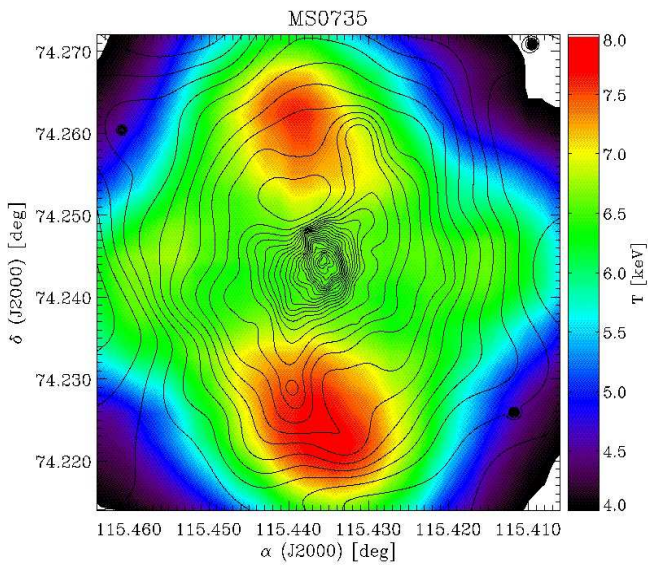


Figure 4 Temperature map of the central 200×200 arcsec of the cluster. Redder colors indicate hotter temperatures. The logarithmically spaced contours, ranging in surface brightness from $1\sigma = 1.0^{-4}$ $\text{cnt s}^{-1} \text{cm}^{-2} \text{pix}^{-2}$ to 100σ , show the locations of the cavities. The hottest regions are at the tips of the cavities, where the shocks are strongest.